



Exploring the severe winter haze in Beijing

G. J. Zheng et al.

This discussion paper is/has been under review for the journal Atmospheric Chemistry and Physics (ACP). Please refer to the corresponding final paper in ACP if available.

Exploring the severe winter haze in Beijing

G. J. Zheng¹, F. K. Duan¹, Y. L. Ma¹, Y. Cheng¹, B. Zheng¹, Q. Zhang^{2,6},
T. Huang³, T. Kimoto³, D. Chang⁴, H. Su⁴, U. Pöschl⁴, Y. F. Cheng⁴, and
K. B. He^{1,5,6}

¹State Key Joint Laboratory of Environment Simulation and Pollution Control, School of Environment, Tsinghua University, Beijing 100084, China

²Ministry of Education Key Laboratory for Earth System Modeling, Center for Earth System Science, Tsinghua University, Beijing 100084, China

³Kimoto Electric Co., Ltd, 3-1 Funahashi-cho Tennoji-ku, Osaka 543-0024, Japan

⁴Multiphase Chemistry Department, Max Planck Institute for Chemistry, 55128, Mainz, Germany

⁵State Environmental Protection Key Laboratory of Sources and Control of Air Pollution Complex, Beijing 100084, China

⁶Collaborative Innovation Center for Regional Environmental Quality, Beijing 100084, China

Title Page

Abstract

Introduction

Conclusions

References

Tables

Figures



Back

Close

Full Screen / Esc

Printer-friendly Version

Interactive Discussion



Received: 16 April 2014 – Accepted: 23 June 2014 – Published: 3 July 2014

Correspondence to: K. B. He (hekb@mail.tsinghua.edu.cn) and
Y. F. Cheng (yafang.cheng@mpic.de)

Published by Copernicus Publications on behalf of the European Geosciences Union.

ACPD

14, 17907–17942, 2014

Exploring the severe winter haze in Beijing

G. J. Zheng et al.

Title Page

Abstract

Introduction

Conclusions

References

Tables

Figures



Back

Close

Full Screen / Esc

Printer-friendly Version

Interactive Discussion



Abstract

Extreme haze episodes repeatedly shrouded Beijing during the winter of 2012–2013, causing major environmental and health problems. To better understand these extreme events, we analyzed the hourly observation data of PM_{2.5} and its major chemical composition, with support of model simulations. Severe winter haze was shown to result from stable synoptic meteorological conditions over a large part of northeastern China, rather than from an abrupt increase in emissions. Build-up of secondary species, including organics, sulfate, nitrate, and ammonium, was the major driving force behind these polluted periods. The contribution of organic matter decreased with increasing pollution level while sulfate and nitrate contributions increased. Correspondingly, the ratio of secondary organic carbon to elemental carbon decreased and had a stable diurnal pattern during heavily polluted periods, indicating weakened photochemical activity due to the dimming effect of high loading of aerosol particles. Under such conditions, the strong increase in sulfate and nitrate contributions to PM_{2.5} was attributed to an elevated conversion ratio, reflecting more active heterogeneous reactions with gradually increasing relative humidity. Moreover, we found that high aerosol concentration was a regional phenomenon. The accumulation process of aerosol particles occurred successively from southeast cities to Beijing. The “apparent” sharp increase in PM_{2.5} concentration of up to several hundred $\mu\text{g m}^{-3}$ per hour recorded in Beijing represented rapid “recovery” from an “interruption” to the continuous pollution accumulation over the region, rather than purely local chemical production. This suggests that regional transport of pollutants played an important role during these severe pollution events.

1 Introduction

Severe haze episodes in the winter of 2012–2013 engulfed Beijing, as well as other cities in southeastern China, causing one of the worst atmospheric pollution events

ACPD

14, 17907–17942, 2014

Exploring the severe winter haze in Beijing

G. J. Zheng et al.

Title Page

Abstract

Introduction

Conclusions

References

Tables

Figures



Back

Close

Full Screen / Esc

Printer-friendly Version

Interactive Discussion



Exploring the severe winter haze in Beijing

G. J. Zheng et al.

Title Page

Abstract

Introduction

Conclusions

References

Tables

Figures



Back

Close

Full Screen / Esc

Printer-friendly Version

Interactive Discussion



in history. With hourly fine particle ($PM_{2.5}$) concentrations up to $\sim 900 \mu\text{g m}^{-3}$, outdoor exposure caused adverse health effects (Nel, 2005; Pöschl, 2005; Peplow, 2014), including severe respiratory system related symptoms and deceases (Cao et al., 2014; Ouyang, 2013). Meanwhile the visibility was reduced down to 100 m, which disrupted traffic with canceled flights and closed highways. The government had to adopt emergency response measures to deal with these pollution episodes (<http://english.sina.com/china/p/2013/0113/548263.html>). In addition to massive amounts of primary particulate matter, high emissions in China provided plenty of gas pollutants to serve as precursors for secondary aerosols (Zhang et al., 2009). Densely distributed mega-cities (i.e., city clusters) have worsened this situation, contributing to regional air pollution. Once the regional pollution is formed, the advection becomes less effective in scavenging local pollutants (no clean air from upwind). Thus, the regional pollution is more persistent compared with air pollution within a specific city. Moreover, cities within this region could not eliminate their pollution solely by reducing local emissions (Chan and Yao, 2008).

These extreme haze episodes attracted great scientific interest. Regional transport of pollutants was found to contribute considerably to concentrations of $PM_{2.5}$ (Z. Wang et al., 2014; L. T. Wang et al., 2014), dust (Yang et al., 2013; Y. Wang et al., 2014), and SO_2 (Yang et al., 2013) in Beijing. Atmospheric dynamic processes during hazy conditions were different from clean conditions, with a significant two-way feedback between $PM_{2.5}$ and boundary layer evolution (Z. Wang et al., 2014). Secondary inorganic aerosol species were suggested to be the major contributor to severe haze, based on off-line $PM_{2.5}$ analysis (Quan et al., 2014), and on-line non-refractory PM_1 analysis by an Aerosol Chemical Speciation Monitor (Sun et al., 2014). In addition, some studies described unusual atmospheric phenomena taking place under heavily polluted conditions, such as extremely low ozone concentration (less than 5 ppb) in the absence of diurnal variation (Zhao et al., 2013) and the synergistic oxidation of SO_2 and NO_2 (He et al., 2014). These findings suggest need for a better understanding on the haze formation mechanisms.

Exploring the severe winter haze in Beijing

G. J. Zheng et al.

Title Page

Abstract

Introduction

Conclusions

References

Tables

Figures

◀

▶

◀

▶

Back

Close

Full Screen / Esc

Printer-friendly Version

Interactive Discussion



In this study, we tried to address the following questions for the winter haze episodes aforementioned: (1) the relative importance of enhanced emission vs. meteorology; (2) the causes of the sharp $PM_{2.5}$ increase during the haze episodes in Beijing, whether it was mainly driven by an extremely rapid local chemical production or by regional transport; and (3) the dominant chemical mechanisms of haze formation.

2 Experimental methods

On-line ambient observation was conducted from 1–31 January 2013 on the campus of Tsinghua University. The observation site is situated on the rooftop of the Environmental Science Building ($40^{\circ}00'17''$ N, $116^{\circ}19'34''$ E), approximately 10 m above ground. Tsinghua University is located in the northwest part of urban Beijing, close to the North 4th Ring Road, without any major pollution sources nearby. All observation data are hourly unified data.

Mass concentrations of fine ($PM_{2.5}$) and coarse ($PM_{2.5-10}$) particles were simultaneously measured based on the β -ray absorption method by a PM-712 Monitor (Kimoto Electric Co., Ltd., Japan), which was equipped with a US-EPA PM_{10} inlet and a $PM_{2.5}$ virtual impactor (Kimoto Electric Co., Ltd., 2012; Kaneyasu et al., 2014). Dehumidification was achieved with the hygroscopic growth correction formula:

$$\text{Dehumidified } PM_{2.5} \text{ mass conc.} = \text{Measured } PM_{2.5} \text{ mass conc.} \times \frac{1}{1 + 0.010 \times e^{6.000 \frac{RH}{100}}} \quad (1)$$

where the 0.010 and 6.000 are localized coefficients, and RH is relative humidity in %. All $PM_{2.5}$ hereinafter refer to the dehumidified $PM_{2.5}$ data.

A Sunset Model 4 semi-continuous carbon analyzer (Beaverton, OR, USA) was used to measure hourly organic carbon (OC) and elemental carbon (EC) concentrations in $PM_{2.5}$. A NIOSH (National Institute for Occupational Safety and Health) temperature protocol was used and the calculation discrepancy under high ambient concentrations

Exploring the severe winter haze in Beijing

G. J. Zheng et al.

Title Page

Abstract

Introduction

Conclusions

References

Tables

Figures



Back

Close

Full Screen / Esc

Printer-friendly Version

Interactive Discussion



was corrected accordingly (G. J. Zheng et al., 2014). OM was estimated as $1.6 \cdot \text{OC}$, based on previous results (Zhang et al., 2014; Xing et al., 2013). The use of fixed OM/OC ratio requires caveats because the ratio might change due to the variable oxidation degree of OM under different conditions.

Hourly sulfate and nitrate concentrations in $\text{PM}_{2.5}$ were measured using an ACSA-08 Monitor (Kimoto Electric Co., Ltd., Japan). The ACSA-08 Monitor measured nitrates using an ultra-violet spectrophotometric method, and quantified sulfates with the BaSO_4 -based turbidimetric method after addition of BaCl_2 dissolved in polyvinyl pyrrolidone solution (Kimoto et al., 2013). Ammonium was predicted under the assumption that it existed as NH_4NO_3 and $(\text{NH}_4)_2\text{SO}_4$ (He et al., 2012), which might be an overestimation based on the non-refractory PM_1 results (Sun et al., 2014). Thus the predicted ammonium given here should be regarded as an upper limit.

An automatic meteorological observation instrument (Milos520, VAISALA Inc., Finland) was used to obtain meteorological parameters, including atmospheric pressure, temperature, RH, wind speed, and wind direction. Specific humidity was calculated from these measured parameters (<http://www.srh.noaa.gov/epz/?n=wxcalc>).

SO_2 and NO_2 concentrations in Beijing, and $\text{PM}_{2.5}$ concentrations in other cities were acquired from the Atmospheric Environment Monitoring Network (Tang et al., 2012). Daily averaged solar radiation reaching ground data were downloaded from the China Meteorological Data Sharing Service System (<http://cdc.cma.gov.cn>). Planetary boundary layer (PBL) height was simulated with the Weather Research & Forecasting Model (B. Zheng et al., 2014).

3 General characteristics of Beijing winter haze

Primary atmospheric pollutant in Beijing during the winter of 2012–2013 was $\text{PM}_{2.5}$, which constituted about 70% of PM_{10} . This ratio increased when $\text{PM}_{2.5}$ pollution became worse (Fig. 1b). Monthly average $\text{PM}_{2.5}$ concentration reached $121.0 \mu\text{g m}^{-3}$ in January 2013, and hourly $\text{PM}_{2.5}$ concentrations peaked at $855.10 \mu\text{g m}^{-3}$, which was

Exploring the severe winter haze in Beijing

G. J. Zheng et al.

Title Page

Abstract

Introduction

Conclusions

References

Tables

Figures



Back

Close

Full Screen / Esc

Printer-friendly Version

Interactive Discussion



the highest ever reported in Beijing (Zhao et al., 2009, 2011, 2013; Zhang et al., 2014). The severe $\text{PM}_{2.5}$ pollution lasted nearly the whole month, characterized by frequent and long-lasting pollution episodes. Here, we define an episode as a set of continuous days with daily $\text{PM}_{2.5}$ averages exceeding $75 \mu\text{g m}^{-3}$. In total, four episodes were identified in January 2013 (Fig. 1a): 4–8 January (Episode I), 10–16 January (Episode II), 18–23 January (Episode III), and 25–31 January (Episode IV). Maximum episode-averaged $\text{PM}_{2.5}$ concentrations reached $245.4 \mu\text{g m}^{-3}$ in Episode II (see Table 1 for comparative information on Episodes I to III; Episode IV was not included because of missing data). In addition to the high average concentrations, these episodes were frequent (intervals between episodes were all ~ 1 day) and long-lasting (5–7 days) compared with typical durations (5 days) and frequencies (1–3 days) of previous Beijing winter haze episodes (Jia et al., 2008).

Another unique feature of the $\text{PM}_{2.5}$ mass concentrations during this winter haze period was their dramatic hourly fluctuation. The maximum daily variation was $778.6 \mu\text{g m}^{-3}$ on 12 January. Hourly $\text{PM}_{2.5}$ changes of over $100 \mu\text{g m}^{-3}$ (increases or decreases) were observed over 40 times during this haze period. Hourly increases or decreases could reach up to $351.8 \mu\text{g m}^{-3}$ and $-217.7 \mu\text{g m}^{-3}$, respectively. Causes of these sharp transitions are discussed in Sect. 5.

The variation of chemical composition with $\text{PM}_{2.5}$ pollution level, and among episodes, was also explored. We classified $\text{PM}_{2.5}$ pollution into 4 categories according to the Air Quality Index (http://kjs.mep.gov.cn/hjbhbz/bzwb/dqhjbh/jcgfffbz/201203/t20120302_224166.htm?COLLCC=2906016564&) (Fig. 1b): clean ($\text{PM}_{2.5} \leq 35 \mu\text{g m}^{-3}$), slightly polluted ($35 < \text{PM}_{2.5} \leq 115 \mu\text{g m}^{-3}$), polluted ($115 < \text{PM}_{2.5} \leq 350 \mu\text{g m}^{-3}$), and heavily polluted ($\text{PM}_{2.5} > 350 \mu\text{g m}^{-3}$), where $\text{PM}_{2.5}$ refers to the hourly concentration. Under this classification, the slightly polluted, polluted, and heavily polluted levels generally correspond to small, moderate, and large $\text{PM}_{2.5}$ peaks in Fig. 1b. With increasing pollution level, the EC fraction decreased slightly, OC fraction decreased significantly, while sulfate and nitrate contributions increased sharply (Fig. 2a). It suggests that secondary inorganic aerosol species

Exploring the severe winter haze in Beijing

G. J. Zheng et al.

Title Page

Abstract

Introduction

Conclusions

References

Tables

Figures



Back

Close

Full Screen / Esc

Printer-friendly Version

Interactive Discussion



become more important during polluted periods concerning its contribution to the $PM_{2.5}$. A similar trend was observed for $NR-PM_1$ (Sun et al., 2014) and off-line samples (Cheng et al., 2014). On average, OC, EC, nitrate, and sulfate comprised 21 %, 3 %, 19 % and 22 % of $PM_{2.5}$ (Fig. 2b). Good correlations with $PM_{2.5}$ were observed for OC, EC and nitrate ($R^2 > 0.8$ for these three species) for all data in January 2013, while for sulfate the correlation became weaker, reflecting larger episodic variations (Fig. 2b). In Episode III, NO_2 exceeded SO_2 by 50 % (Table 1), generally in accordance with previous studies (Meng et al., 2009). In contrast, concentration of SO_2 exceeded NO_2 in Episodes I and II. Compared with Episode II, Episode I was much drier, which is unfavorable to the sulfate formation. The relatively high SO_2 but low NO_2 concentrations in Episodes I and II may indicate the significance of stationary sources (coal combustion, etc.) in local emissions or regional SO_2 -rich air masses transported to Beijing.

4 Emission enhancement vs. synoptic conditions

Haze episodes were much more severe and frequent in winter 2013 than in 2012. One possible explanation is that there was an abrupt emission enhancement during 2013. However, we did not find such change in the emission inventory (<http://www.meicmodel.org/>). Annual average emissions of primary $PM_{2.5}$, SO_2 and NO_x show slight differences between 2013 and 2012 (1.2 %, -1.3 % and 0.8 %, respectively) for the Beijing-Tianjin-Hebei region. The changes of monthly averaged emissions in January were higher than the annual average changes in rates, i.e., 2.1 %, 1.5 % and 2.5 % for primary $PM_{2.5}$, SO_2 , and NO_x , respectively; but they are still not significant compared to the changes in pollutant concentrations. Thus, we suspect that these haze episodes arose from the unfavorable synoptic conditions in January 2013.

The relative importance of enhanced emission vs. unfavorable meteorology was estimated by model simulations with three scenarios (Fig. 3). Base scenario (a) was designed to simulate the actual situation, i.e., with both input emission inventory and

Exploring the severe winter haze in Beijing

G. J. Zheng et al.

[Title Page](#)[Abstract](#)[Introduction](#)[Conclusions](#)[References](#)[Tables](#)[Figures](#)[⏪](#)[⏩](#)[◀](#)[▶](#)[Back](#)[Close](#)[Full Screen / Esc](#)[Printer-friendly Version](#)[Interactive Discussion](#)

meteorology for January 2013. In scenarios (b) and (c), 2012 meteorology and 2012 emission inventory data were used, respectively. Our model used the Weather Research and Forecasting Model (version 3.5.1) and the Community Multiscale Air Quality (CMAQ, version 5.0.1) modeling system. The CMAQ model was enhanced with more comprehensive heterogeneous reactions (Wang et al., 2012) to improve its performance for sulfate and nitrate simulations. Details of our model configuration, modifications, and its evaluation are described in B. Zheng et al. (2014).

As expected, the influence of emission difference was negligible (Fig. 3a and 3c), resulting in a $PM_{2.5}$ difference of within $\pm 10 \mu g m^{-3}$ for the North China Plain (NCP) (Fig. 3e). The negligible influence of variation in emissions was corroborated by excellent correlation between scenarios (a) and (c) in the simulated $PM_{2.5}$ results for Beijing ($R^2 = 0.97$).

In contrast, stable synoptic conditions in January 2013, which favored accumulation of emitted pollutants, were essential to the formation of the severe regional haze. Under the same emission level, changing the meteorological conditions from 2012 to 2013 resulted in a monthly average $PM_{2.5}$ increase of 10–40 $\mu g m^{-3}$ in the Beijing area, and up to 120 $\mu g m^{-3}$ over the whole NCP (Fig. 3a, b, d). This suggests that the severe haze episodes in January 2013 were most likely due to unfavorable meteorology, rather than an abrupt increase in emissions (Fig. 3d, e).

Figure 4 compares peak $PM_{2.5}$ concentrations in the NCP region during Episodes II to IV and their corresponding surface weather maps, together with surface weather map from a clean hour (Fig. 4g). During severe haze episodes, the regional pollution covered most of Hebei and northern Henan Provinces. In general, Shandong Province was less polluted, except during Episode IV. Beijing borders this polluted region, with mountains to the northwest. Surface weather maps from polluted periods were generally characterized by a weak high-pressure center (1034–1037 hPa) north-east of Beijing, which could result in low surface wind speed and prevent the influx of northwest clean air (Xu et al., 2011; Zhao et al., 2013). During the peak hours of Episode II, Beijing was located near a low-pressure trough, where air masses from

Exploring the severe winter haze in Beijing

G. J. Zheng et al.

Title Page

Abstract

Introduction

Conclusions

References

Tables

Figures



Back

Close

Full Screen / Esc

Printer-friendly Version

Interactive Discussion



south, west and northeast converged. During Episode III, Beijing was located in a saddle between two pairs of high- and low-pressure centers, which also led to enhanced stability. In contrast, weather patterns for the clean hours were characterized by strong high-pressure centers (up to 1046 hPa) northwest of Beijing, i.e., the Siberian Anticyclone. With sharp pressure gradient, synoptic conditions produce effective convection and strong northerly winds, bringing dry and clean air masses into Beijing.

Local meteorology, controlled by synoptic conditions, could have “deterministic impacts” on air pollution levels (Xu et al., 2011). Compared with the clean periods, the polluted periods were associated with significantly lower wind speed and PBL, and higher temperature and RH (Fig. 5). Besides changes in the average level, diurnal pattern of temperature in polluted periods could also differ from clean periods, with diminished overnight (0:00 to 6:00 a.m.) temperature drop.

5 Local chemical production vs. regional transport

As shown in Fig. 6, Episode II consists of several sharp-increase events, in which $PM_{2.5}$ concentrations increased by over $400 \mu\text{g m}^{-3}$ within 1–3 h (maximum mass growth rate up to $351.8 \mu\text{g m}^{-3} \text{h}^{-1}$). Earlier studies have attributed this dramatic rate of increase to fast local chemical production (Y. Wang et al., 2014). However, we found that the apparent rapid changes are more likely to be caused by the regional transport of clean/polluted air masses. In winter, the Siberian Anticyclone could bring clean air masses into NCP (Jia et al., 2008; Liu et al., 2013) while southerly winds refill the areas with polluted air masses. The transition between clean and polluted air masses may result in an “apparent” sharp build-up of particle concentrations. In other words, these events reflected “interruption” and rapid recovery of pollution from adjacent areas, rather than merely local chemical production.

The impact of transport is supported by the temporal variations in the regional distribution of $PM_{2.5}$ concentrations, the surface weather maps, and the specific humidity (Figs. 6 and 7). The first evidence is that these sharp $PM_{2.5}$ build-up events were unique

Exploring the severe winter haze in Beijing

G. J. Zheng et al.

Title Page

Abstract

Introduction

Conclusions

References

Tables

Figures



Back

Close

Full Screen / Esc

Printer-friendly Version

Interactive Discussion



to Beijing among all the 8 cities around/in the NCP (Fig. 6). Chengde and Zhangjiakou are situated to the north of NCP with mountains in between (Fig. 6a). Among the NCP cities, Beijing is located at the northern tip, with mountains to the north and west shielding the city (Fig. 6a2). When conditions favor transport of clean air from north or northwest (i.e. with the advent of a cold air current), Beijing is the first one among NCP cities to embrace it, which resulted in a sharp drop of $PM_{2.5}$ concentrations. In this case, $PM_{2.5}$ levels in Beijing became similar to the upwind cities, i.e., Chengde and Zhangjiakou (yellow solid circles; Fig. 6b1). However, these cold air currents were too weak to go further, leaving the rest NCP cities unaffected. Not surprisingly, the influence of these weak cold air currents soon receded and the polluted air parcels were transported back to Beijing, which lead to a sharp increase in the $PM_{2.5}$ level similar as the rest NCP cities (e.g., Shijiazhuang, Baoding, Tianjin, Langfang, and Tangshan) (yellow solid circles; Fig. 6b2 and b3).

In accordance with the above description, surface weather maps showed that the sharp $PM_{2.5}$ increase/decrease events in Beijing during January 2013 were always accompanied with quick transition between low/high pressure systems. As shown in Fig. 7b, the two sharp drops in $PM_{2.5}$ concentration on 11 and 12 January corresponded to a weak high-pressure system developed in the mountains northwest of Beijing, which brought clean air mass into the city. When the high-pressure systems diminished, a low-pressure system developed southwest of Beijing, and the air mass in Beijing was again affected by the regional background pollution, resulting in a sharp increase in $PM_{2.5}$ concentration.

The observed variation of the specific humidity, an indicator for the origin of air masses (Jia et al., 2008), also supports our explanation (Fig. 7a). Air masses from the south were usually warmer and wetter than the northern air masses, thus possessing a higher specific humidity. During the rapid changes of $PM_{2.5}$, the trend of specific humidity nicely followed the variations of $PM_{2.5}$ (Fig. 7a, pink and yellow rectangles marked periods), which reflected the quick transition of air parcel origins. It has been suggested that the decrease of PBL height will compress air pollutants into a shallow

Exploring the severe winter haze in Beijing

G. J. Zheng et al.

Title Page

Abstract

Introduction

Conclusions

References

Tables

Figures



Back

Close

Full Screen / Esc

Printer-friendly Version

Interactive Discussion



layer, resulting in elevated pollution levels (Liu et al., 2013). However, our results indicated that the compression was not really happening. Rather, the decrease of PBL height hindered the vertical mixing of pollutants, resulting in a faster accumulation and higher concentrations. As shown in Fig. 7a, the time lag between variations in PBL and its effects on $\text{PM}_{2.5}$ concentration is a clear evidence demonstrating that the PBL was not “compressing” air pollutants into a shallower layer. Otherwise, concurrent increase in $\text{PM}_{2.5}$ will be found during the decrease of PBL height.

6 Formation of secondary aerosols

Compared with clean conditions, the hazy days are characteristic of weaker radiation and higher RH. The RH depends on the synoptic conditions while the radiation reduction is due to the direct radiative effects of aerosol particles (Crutzen and Birks, 1982; Ramanathan and Carmichael, 2008; Ramanathan et al., 2001; Cheng et al., 2008; Wendisch et al., 2008). Secondary aerosols (inorganic and organic) are major components in fine particles in China (Yang et al., 2011). In this section, we will evaluate the impact of changes in radiation and RH on the formation of secondary aerosols.

6.1 Weakened photochemistry

The radiative forcing imposed by aerosol particles is particularly strong during haze episodes in Beijing because of extremely high particle concentrations. During haze episodes, the amount of solar radiation reaching the ground was low (down to 2.77 MJ m^{-2} , 13 January) (Fig. 8a), rendering high photochemical activity impossible. The reduction of radiation intensities will change the atmospheric photochemistry and oxidant concentrations (hydroxyl radical (OH) and ozone (O_3)), which will consequently change the production and aging of secondary organic aerosols (SOA) (Hallquist et al., 2009; Jimenez et al., 2009).

Exploring the severe winter haze in Beijing

G. J. Zheng et al.

Title Page

Abstract

Introduction

Conclusions

References

Tables

Figures



Back

Close

Full Screen / Esc

Printer-friendly Version

Interactive Discussion



Usually, we can tell the increase of SOA formation from its elevated concentrations. During the haze event, however, the reduced boundary layer height (dilution/mixing effect) itself is already enough to increase pollutant concentrations. For example, concentrations of EC, which is merely of primary origin, continuously increased from clean to heavily polluted conditions (Fig. 8b1). Therefore, we used the ratio of OC to EC to account for the boundary layer effect. Though OC concentrations increased with pollution levels (Fig. 8b2), the OC/EC ratios show a decreasing trend as air pollution become more severe (Fig. 8b5). Compared to OC/EC of 10.8 under clean conditions, the ratios decrease to 6.7 ~ 7.4 for polluted conditions. Such decreasing trend suggests that the radiation attenuation suppressed SOA formation.

Besides the total OC concentrations, investigations of secondary organic carbon (SOC) lead to the same conclusion. The SOC was estimated using the EC-tracer method (Lim and Turpin, 2002). Briefly, SOC was estimated using these formulae:

$$\text{Primary OC} = \text{EC} \cdot (\text{OC/EC})_{\text{pri}} + N \quad (2)$$

$$\text{SOC} = \text{OC} - \text{Primary OC} \quad (3)$$

The basic assumptions and underlying principles of this method are discussed in Lim and Turpin (2002) and Lin et al. (2009). In our study, data pairs with the lowest 10 % percentile of ambient OC/EC ratios were used to estimate the primary OC/EC ratio (Fig. 9a). York regression (York et al., 2004) was used to estimate the intercept N and the slope, i.e., values of $(\text{OC/EC})_{\text{pri}}$, according to Saylor et al. (2006).

The SOC/OC ratio dropped from 30 % under clean conditions to 15 % during heavily polluted periods, suggesting a reduced production rate due to weakened photochemical activity. The relatively small proportion of SOC in total OC (~ 30 %, Fig. 9b) also supported weakened photochemical activity during haze episodes. This estimation was consistent with those from off-line $\text{PM}_{2.5}$ samples from winter 2009 (~ 32 %, Cheng et al., 2011), and positive matrix factorization-resolved NR-PM_1 samples in winter 2011–2012 (~ 31 %, Sun et al., 2013b). Overall, the SOC to OC ratio during haze

episodes was much lower than that recorded in summer (roughly 50%; Cheng et al., 2014).

Moreover, changes in the diurnal profile of SOC/EC with pollution level (Fig. 8b6) also reflected the suppressed SOA formation due to weakened photochemistry. Like OC, SOC was also scaled by EC to account for the boundary layer effect. In clean periods, average diurnal trends in SOC/EC have both an afternoon maximum and a nighttime maximum. These two peaks both diminished as the pollution got worse, and instead a stable diurnal pattern was observed during heavily polluted periods. Decrease in the nighttime SOC/EC peaks could be explained by the more stable night temperatures (and corresponding stable RH) with rising pollution levels (Fig. 5) (Lim and Turpin, 2002), while afternoon SOC/EC peaks were typically associated with photochemical activity. The weakening of the afternoon peak indicated a reduction in photochemical activity.

6.2 Enhanced heterogeneous chemistry

Unlike OM, contributions of sulfate and nitrate to $PM_{2.5}$ were increasing during the haze events (Fig. 2). Again, we used their ratios to EC to account for the boundary layer effect. Significant increase of SO_4^{2-}/EC and NO_3^-/EC ratios were found from clean periods (3.03 and 3.33, respectively) to heavily polluted periods (6.35 and 5.89, respectively), suggesting enhanced chemical productions. The SOR and NOR (molar ratio of sulfate or nitrate to sum of sulfate and SO_2 or nitrate and NO_2) have been used as indicators of secondary transformation (Sun et al., 2006). The fact that SOR and NOR increased much more rapidly than SO_2 and NO_2 as pollutions became more severe (Column 3 in Fig. 10), is another evidence of elevated secondary formations of sulfate and nitrate during severe haze events.

Both gas-phase and heterogeneous reactions could contribute to the formation of sulfate and nitrate from SO_2 and NO_2 , and thus elevating the SOR and NOR. Sulfate is formed through oxidation of SO_2 by gas-phase reactions with OH (Stockwell and Calvert, 1983; Blitz et al., 2003) and stabilized Criegee intermediate (which is formed

Title Page

Abstract

Introduction

Conclusions

References

Tables

Figures



Back

Close

Full Screen / Esc

Printer-friendly Version

Interactive Discussion



Exploring the severe winter haze in Beijing

G. J. Zheng et al.

Title Page

Abstract

Introduction

Conclusions

References

Tables

Figures

◀

▶

◀

▶

Back

Close

Full Screen / Esc

Printer-friendly Version

Interactive Discussion



by O₃ and alkenes) (Mauldin et al., 2012), and by heterogeneous reactions with dissolved H₂O₂ or with O₂ under the catalysis of transition metal (Seinfeld and Pandis, 2006). Nitrate formation is dominated by the gas-phase reaction of NO₂ with OH during daylight, and the heterogeneous reactions of nitrate radical (NO₃) during nighttime (Seinfeld and Pandis, 2006).

As discussed in Sect. 6.1, gas-phase production of sulfate and nitrate is unlikely to be important owing to the weakened photochemistry, which implied low gas-phase oxidant concentrations of OH and ozone (Y. Wang et al., 2014; Zhao et al., 2013). This was further supported by the weak correlation between SOR and temperature (Fig. 11a), for gas-phase SO₂ oxidation by OH radicals was proposed to be strongly correlated with temperature (Seinfeld and Pandis, 2006; Sun et al., 2006; Blitz et al., 2003). Thus we infer that the rapid increase in SOR and NOR during polluted periods (Fig. 10) was mainly due to heterogeneous reactions, especially reactions associated with aerosol water.

Dependence of SOR and NOR on RH (Fig. 11) also supported our inference. Both SOR and NOR were constant under dry conditions (RH < 50 %) (Fig. 11a and b) while started increasing when RH > 50 %, resulting in average values around 0.34 and 0.28 at RH 70–80 %, respectively. This suggests important contributions from heterogeneous reactions with abundant aerosol water under wet conditions (Sun et al., 2013a). The observed SOR value was high compared with previously reported values of 0.24 (Wang et al., 2006) and 0.29 (Zhao et al., 2013) during hazy days in Beijing. The NOR values for this study were higher than spring hazy days in 2001–2004 (0.22; Wang et al., 2006), but significantly lower than for the hazy episode in January 2010 (0.51; Zhao et al., 2013).

Concerning the SOA formation, the contribution of heterogeneous reactions might be possible, but it should be much less significant than for sulfate and nitrate. For RH > 50 %, SO₄²⁻/EC and NO₃⁻/EC ratios rose significantly (Fig. 11d) while SOC/EC ratios remained constant (Fig. 9c). By using HOA (hydrocarbon-like organic aerosol)

instead of EC, Sun et al. (2013a) found similar phenomena. Apparently, SOC does not have a heterogeneous formation pathway as effective as those of sulfate and nitrate.

7 Conclusions

The severe haze pollution during January 2013 was not a Beijing-localized phenomenon. Rather, it was the result of local pollutants superposed on background regional pollution, which affected the whole NCP. Although pollutant emissions were high, there was no abrupt enhancement in 2013. The occurrence of the severe winter haze resulted from stable synoptic meteorological conditions over a large area of northeastern China. Surface weather maps from hazy periods were characterized by a weak high-pressure center northeast of Beijing, while the termination of a haze episode was always accompanied by the Siberian Anticyclone (Xu et al., 2011; Jia et al., 2008; Liu et al., 2013).

Rather than chemical productions, transport of polluted regional air masses was suggested as the key process leading to the sharp increases of aerosols concentrations. Beijing pollution was temporarily flushed away by strong winds associated with the arrival of a weak cold air current, but as its influence weakened, the polluted regional air mass readily reoccupied the Beijing area, resulting in an apparent rapid build-up of $PM_{2.5}$. This hypothesis was supported by data on the $PM_{2.5}$ levels around Beijing, specific humidity and PBL height, as well as surface weather maps.

Atmospheric chemistry and physics during severe haze pollutions are illustrated in a conceptual model (Fig. 12). With the onset of stable synoptic conditions, RH rises, primary pollutants began to accumulate and regional pollution began to form. If the stable conditions last long enough, $PM_{2.5}$ build-up occurs, such that solar radiation is reduced at the ground. This inhibits surface temperature fluctuation, making easier the formation of inversed layer and rendering the atmosphere into a more stable condition. Meanwhile, photochemical activity is weakened under low solar radiation, and secondary aerosol formation via this pathway becomes less important. However, un-

Exploring the severe winter haze in Beijing

G. J. Zheng et al.

Title Page

Abstract

Introduction

Conclusions

References

Tables

Figures



Back

Close

Full Screen / Esc

Printer-friendly Version

Interactive Discussion



Exploring the severe winter haze in Beijing

G. J. Zheng et al.

Title Page

Abstract

Introduction

Conclusions

References

Tables

Figures



Back

Close

Full Screen / Esc

Printer-friendly Version

Interactive Discussion



der high RH, and enhanced precursor concentrations, heterogeneous reactions play a more important role, especially those associated with the aerosol water phase. This results in the rapid build-up of sulfates and nitrates, enhancing PM_{2.5} pollution. The sulfates and nitrates absorb more water into the particulate phase, promoting subsequent heterogeneous reactions. This cycle terminates with the incursion of a strong cold front, usually the Siberian Anticyclone.

Acknowledgements. This work was supported by the National Natural Science Foundation of China (21190054, 21221004, 21107061, and 41222036), China's National Basic Research Program (2010CB951803), and the Japan International Cooperation Agency. F. K. Duan acknowledges support from a National Excellent Doctoral Dissertation of China Award (2007B57). Y. Cheng was supported by the China Postdoctoral Science Foundation (2013T60130 and 2013M540104). D. Chang, H. Su and Y. F. Cheng were supported by the Max Planck Society (MPG), the EU project PEGASOS (265148) and National Natural Science Foundation of China (41330635).

References

- Blitz, M. A., Hughes, K. J., and Pilling, M. J.: Determination of the high-pressure limiting rate coefficient and the enthalpy of reaction for OH + SO₂, *J. Phys. Chem. A*, 107, 1971–1978, doi:10.1021/jp026524y, 2003.
- Cao, C., Jiang, W., Wang, B., Fang, J., Lang, J., Tian, G., Jiang, J., and Zhu, T. F.: Inhalable microorganisms in Beijing's PM_{2.5} and PM₁₀ pollutants during a severe smog event, *Environ. Sci. Technol.*, 48, 1499–1507, 2014.
- Carmichael, G. R., Streets, D. G., Calori, G., Amann, M., Jacobson, M. Z., Hansen, J., and Ueda, H.: Changing trends in sulfur emissions in Asia: implications for acid deposition, air pollution, and climate, *Environ. Sci. Technol.*, 36, 4707–4713, doi:10.1021/es011509c, 2002.
- Chan, C. K. and Yao, X.: Air pollution in mega cities in China, *Atmos. Environ.*, 42, 1–42, 2008.
- Chen, Y., Sheng, G., Bi, X., Feng, Y., Mai, B., and Fu, J.: Emission factors for carbonaceous particles and polycyclic aromatic hydrocarbons from residential coal combustion in China, *Environ. Sci. Technol.*, 39, 1861–1867, 2005.

Exploring the severe winter haze in Beijing

G. J. Zheng et al.

Title Page

Abstract

Introduction

Conclusions

References

Tables

Figures



Back

Close

Full Screen / Esc

Printer-friendly Version

Interactive Discussion



Cheng, Y., Wiedensohler, A., Eichler, H., Heintzenberg, J., Tesche, M., Ansmann, A.,
Wendisch, M., Su, H., Althausen, D., and Herrmann, H.: Relative humidity dependence of
aerosol optical properties and direct radiative forcing in the surface boundary layer at Xinken
in Pearl River Delta of China: an observation based numerical study, *Atmos. Environ.*, 42,
6373–6397, 2008.

Cheng, Y., He, K.-B., Duan, F.-K., Zheng, M., Du, Z.-Y., Ma, Y.-L., and Tan, J.-H.: Ambient
organic carbon to elemental carbon ratios: influences of the measurement methods and
implications, *Atmos. Environ.*, 45, 2060–2066, doi:10.1016/j.atmosenv.2011.01.064, 2011.

Cheng, Y., He, K.-B., Duan, F.-K., Du, Z.-Y., Zheng, M., and Ma, Y.-L.: Ambient organic car-
bon to elemental carbon ratios: influence of the thermal–optical temperature protocol and
implications, *Sci. Total Environ.*, 468, 1103–1111, 2014.

Crutzen, P. J. and Birks, J. W.: Atmosphere after a nuclear war: twilight at noon, *Ambio*, 11,
114–125, 1982.

Docherty, K. S., Stone, E. A., Ulbrich, I. M., DeCarlo, P. F., Snyder, D. C., Schauer, J. J.,
Peltier, R. E., Weber, R. J., Murphy, S. M., Seinfeld, J. H., Grover, B. D., Eatough, D. J.,
and Jimenez, J. L.: Apportionment of primary and secondary organic aerosols in Southern
California during the 2005 Study of Organic Aerosols in Riverside (SOAR-1), *Environ. Sci.
Technol.*, 42, 7655–7662, doi:10.1021/es8008166, 2008.

Duan, J., Tan, J., Yang, L., Wu, S., and Hao, J.: Concentration, sources and ozone formation
potential of volatile organic compounds (VOCs) during ozone episode in Beijing, *Atmos.
Res.*, 88, 25–35, doi:10.1016/j.atmosres.2007.09.004, 2008.

Hallquist, M., Wenger, J. C., Baltensperger, U., Rudich, Y., Simpson, D., Claeys, M., Dom-
men, J., Donahue, N. M., George, C., Goldstein, A. H., Hamilton, J. F., Herrmann, H., Hoff-
mann, T., Iinuma, Y., Jang, M., Jenkin, M. E., Jimenez, J. L., Kiendler-Scharr, A., Maen-
haut, W., McFiggans, G., Mentel, Th. F., Monod, A., Prévôt, A. S. H., Seinfeld, J. H., Sur-
ratt, J. D., Szmigielski, R., and Wildt, J.: The formation, properties and impact of sec-
ondary organic aerosol: current and emerging issues, *Atmos. Chem. Phys.*, 9, 5155–5236,
doi:10.5194/acp-9-5155-2009, 2009.

He, H., Wang, Y., Ma, Q., Ma, J., Chu, B., Ji, D., Tang, G., Liu, C., Zhang, H., and Hao, J.:
Mineral dust and NO_x promote the conversion of SO_2 to sulfate in heavy pollution days, *Sci.
Rep.*, 4, 4172, doi:10.1038/srep04172, 2014.

He, K., Zhao, Q., Ma, Y., Duan, F., Yang, F., Shi, Z., and Chen, G.: Spatial and seasonal vari-
ability of $\text{PM}_{2.5}$ acidity at two Chinese megacities: insights into the formation of secondary

inorganic aerosols, *Atmos. Chem. Phys.*, 12, 1377–1395, doi:10.5194/acp-12-1377-2012, 2012.

Jia, Y., Rahn, K. A., He, K., Wen, T., and Wang, Y.: A novel technique for quantifying the regional component of urban aerosol solely from its sawtooth cycles, *J. Geophys. Res.*, 113, D21309, doi:10.1029/2008jd010389, 2008.

Jimenez, J. L., Canagaratna, M. R., Donahue, N. M., Prevot, A. S. H., Zhang, Q., Kroll, J. H., DeCarlo, P. F., Allan, J. D., Coe, H., Ng, N. L., Aiken, A. C., Docherty, K. S., Ulbrich, I. M., Grieshop, A. P., Robinson, A. L., Duplissy, J., Smith, J. D., Wilson, K. R., Lanz, V. A., Hueglin, C., Sun, Y. L., Tian, J., Laaksonen, A., Raatikainen, T., Rautiainen, J., Vaattovaara, P., Ehn, M., Kulmala, M., Tomlinson, J. M., Collins, D. R., Cubison, M. J., Dunlea, E. J., Huffman, J. A., Onasch, T. B., Alfarra, M. R., Williams, P. I., Bower, K., Kondo, Y., Schneider, J., Drewnick, F., Borrmann, S., Weimer, S., Demerjian, K., Salcedo, D., Cottrell, L., Griffin, R., Takami, A., Miyoshi, T., Hatakeyama, S., Shimono, A., Sun, J. Y., Zhang, Y. M., Dzepina, K., Kimmel, J. R., Sueper, D., Jayne, J. T., Herndon, S. C., Trimborn, A. M., Williams, L. R., Wood, E. C., Middlebrook, A. M., Kolb, C. E., Baltensperger, U., and Worsnop, D. R.: Evolution of organic aerosols in the atmosphere, *Science*, 326, 1525–1529, doi:10.1126/science.1180353, 2009.

Kaneyasu, N., Yamamoto, S., Sato, K., Takami, A., Hayashi, M., Hara, K., Kawamoto, K., Okuda, T., and Hatakeyama, S.: Impact of long-range transport of aerosols on the PM_{2.5} composition at a major metropolitan area in the northern Kyushu area of Japan, *Atmos. Environ.*, doi:10.1016/j.atmosenv.2014.01.029, in press, 2014.

Khalil, M. A. K. and Rasmussen, R. A.: Tracers of wood smoke, *Atmos. Environ.*, 37, 1211–1222, doi:10.1016/s1352-2310(02)01014-2, 2003.

Kimoto Electric Co., Ltd.: Technical Notes for Continuous Measuring Methods for Atmospheric Suspended Particulate Matters, 3rd edn., March 2012, Osaka, Japan, 2012 (in Japanese).

Kimoto, H., Ueda, A., Tsujimoto, K., Mitani, Y., Toyazaki, Y., and Kimoto, T.: Development of a continuous dichotomous aerosol chemical speciation analyzer, *Clean Technology*, 23, 49–52, 2013, in Japanese.

Lim, H.-J. and Turpin, B. J.: Origins of primary and secondary organic aerosol in Atlanta: results of time-resolved measurements during the Atlanta supersite experiment, *Environ. Sci. Technol.*, 36, 4489–4496, 2002.

Lin, P., Hu, M., Deng, Z., Slanina, J., Han, S., Kondo, Y., Takegawa, N., Miyazaki, Y., Zhao, Y., and Sugimoto, N.: Seasonal and diurnal variations of organic carbon in PM_{2.5} in Bei-

Exploring the severe winter haze in Beijing

G. J. Zheng et al.

Title Page

Abstract

Introduction

Conclusions

References

Tables

Figures



Back

Close

Full Screen / Esc

Printer-friendly Version

Interactive Discussion



Exploring the severe winter haze in Beijing

G. J. Zheng et al.

[Title Page](#)[Abstract](#)[Introduction](#)[Conclusions](#)[References](#)[Tables](#)[Figures](#)[Back](#)[Close](#)[Full Screen / Esc](#)[Printer-friendly Version](#)[Interactive Discussion](#)

jing and the estimation of secondary organic carbon, *J. Geophys. Res.*, 114, D00G11, doi:10.1029/2008jd010902, 2009.

Liu, X. G., Li, J., Qu, Y., Han, T., Hou, L., Gu, J., Chen, C., Yang, Y., Liu, X., Yang, T., Zhang, Y., Tian, H., and Hu, M.: Formation and evolution mechanism of regional haze: a case study in the megacity Beijing, China, *Atmos. Chem. Phys.*, 13, 4501–4514, doi:10.5194/acp-13-4501-2013, 2013.

Lu, K. D., Hofzumahaus, A., Holland, F., Bohn, B., Brauers, T., Fuchs, H., Hu, M., Häseler, R., Kita, K., Kondo, Y., Li, X., Lou, S. R., Oebel, A., Shao, M., Zeng, L. M., Wahner, A., Zhu, T., Zhang, Y. H., and Rohrer, F.: Missing OH source in a suburban environment near Beijing: observed and modelled OH and HO₂ concentrations in summer 2006, *Atmos. Chem. Phys.*, 13, 1057–1080, doi:10.5194/acp-13-1057-2013, 2013.

Mauldin, R. L., Berndt, T., Sipila, M., Paasonen, P., Petaja, T., Kim, S., Kurten, T., Stratmann, F., Kerminen, V. M., and Kulmala, M.: A new atmospherically relevant oxidant of sulphur dioxide, *Nature*, 488, 193–196, doi:10.1038/nature11278, 2012.

Meng, Z. Y., Xu, X. B., Yan, P., Ding, G. A., Tang, J., Lin, W. L., Xu, X. D., and Wang, S. F.: Characteristics of trace gaseous pollutants at a regional background station in Northern China, *Atmos. Chem. Phys.*, 9, 927–936, doi:10.5194/acp-9-927-2009, 2009.

Nel, A.: Air pollution-related illness: effects of particles, *Science*, 308, 804–806, 2005.

Ouyang, Y.: China wakes up to the crisis of air pollution, *The Lancet Respiratory Medicine*, 1, p. 12, doi:10.1016/S2213-2600(12)70065-6, 2013.

Peplow, M.: Beijing smog contains witches' brew of microbes, *Nature*, doi:10.1038/nature.2014.14640, 2014.

Pöschl, U.: Atmospheric aerosols: composition, transformation, climate and health effects, *Angew. Chem. Int. Edit.*, 44, 7520–7540, 2005.

Plaza, J., Gomez-Moreno, F. J., Nunez, L., Pujadas, M., and Artinano, B.: Estimation of secondary organic aerosol formation from semicontinuous OC-EC measurements in a Madrid suburban area, *Atmos. Environ.*, 40, 1134–1147, doi:10.1016/j.atmosenv.2005.11.007, 2006.

Quan, J., Tie, X., Zhang, Q., Liu, Q., Li, X., Gao, Y., and Zhao, D.: Characteristics of heavy aerosol pollution during the 2012–2013 winter in Beijing, China, *Atmos. Environ.*, 88, 83–89, doi:10.1016/j.atmosenv.2014.01.058, 2014.

Ramanathan, V. and Carmichael, G.: Global and regional climate changes due to black carbon, *Nat. Geosci.*, 1, 221–227, 2008.

Exploring the severe winter haze in Beijing

G. J. Zheng et al.

Title Page

Abstract

Introduction

Conclusions

References

Tables

Figures



Back

Close

Full Screen / Esc

Printer-friendly Version

Interactive Discussion



Ramanathan, V., Crutzen, P. J., Lelieveld, J., Mitra, A., Althausen, D., Anderson, J., Andreae, M., Cantrell, W., Cass, G., and Chung, C.: Indian Ocean Experiment: an integrated analysis of the climate forcing and effects of the great Indo–Asian haze, *J. Geophys. Res.*, 106, 28371–28398, 2001.

5 Saylor, R. D., Edgerton, E. S., and Hartsell, B. E.: Linear regression techniques for use in the EC tracer method of secondary organic aerosol estimation, *Atmos. Environ.*, 40, 7546–7556, doi:10.1016/j.atmosenv.2006.07.018, 2006.

Seinfeld, J. H. and Pandis, S. N.: *Atmospheric Chemistry and Physics: from Air Pollution to Climate Change*, 2nd edn., John Wiley and Sons, Inc., Hoboken, NJ, 2006.

10 Stockwell, W. R. and Calvert, J. G.: The mechanism of the HO-SO₂ reaction, *Atmos. Environ.*, 17, 2231–2235, doi:10.1016/0004-6981(83)90220-2, 1983.

Sun, Y., Zhuang, G., Tang, A., Wang, Y., and An, Z.: Chemical characteristics of PM_{2.5} and PM₁₀ in haze-fog episodes in Beijing, *Environ. Sci. Technol.*, 40, 3148–3155, 2006.

15 Sun, Y., Wang, Z., Fu, P., Jiang, Q., Yang, T., Li, J., and Ge, X.: The impact of relative humidity on aerosol composition and evolution processes during wintertime in Beijing, China, *Atmos. Environ.*, 77, 927–934, 2013a.

Sun, Y. L., Wang, Z. F., Fu, P. Q., Yang, T., Jiang, Q., Dong, H. B., Li, J., and Jia, J. J.: Aerosol composition, sources and processes during wintertime in Beijing, China, *Atmos. Chem. Phys.*, 13, 4577–4592, doi:10.5194/acp-13-4577-2013, 2013b.

20 Sun, Y., Jiang, Q., Wang, Z., Fu, P., Li, J., Yang, T., and Yin, Y.: Investigation of the sources and evolution processes of severe haze pollution in Beijing in January 2013, *J. Geophys. Res.*, 119, 4380–4398, 2014.

Tang, G., Wang, Y., Li, X., Ji, D., Hsu, S., and Gao, X.: Spatial-temporal variations in surface ozone in Northern China as observed during 2009–2010 and possible implications for future air quality control strategies, *Atmos. Chem. Phys.*, 12, 2757–2776, doi:10.5194/acp-12-2757-2012, 2012.

25 Wang, K., Zhang, Y., Nenes, A., and Fountoukis, C.: Implementation of dust emission and chemistry into the Community Multiscale Air Quality modeling system and initial application to an Asian dust storm episode, *Atmos. Chem. Phys.*, 12, 10209–10237, doi:10.5194/acp-12-10209-2012, 2012.

30 Wang, L. T., Wei, Z., Yang, J., Zhang, Y., Zhang, F. F., Su, J., Meng, C. C., and Zhang, Q.: The 2013 severe haze over southern Hebei, China: model evaluation, source apportionment, and

Exploring the severe winter haze in Beijing

G. J. Zheng et al.

Title Page

Abstract

Introduction

Conclusions

References

Tables

Figures



Back

Close

Full Screen / Esc

Printer-friendly Version

Interactive Discussion



policy implications, *Atmos. Chem. Phys.*, 14, 3151–3173, doi:10.5194/acp-14-3151-2014, 2014.

Wang, Y., Zhuang, G., Sun, Y., and An, Z.: The variation of characteristics and formation mechanisms of aerosols in dust, haze, and clear days in Beijing, *Atmos. Environ.*, 40, 6579–6591, 2006.

Wang, Y., Yao, L., Wang, L., Liu, Z., Ji, D., Tang, G., Zhang, J., Sun, Y., Hu, B., and Xin, J.: Mechanism for the formation of the January 2013 heavy haze pollution episode over central and eastern China, *Sci. China Earth Sci.*, 57, 14–25, 2014.

Wang, Z., Li, J., Wang, Z., Yang, W., Tang, X., Ge, B., Yan, P., Zhu, L., Chen, X., and Chen, H.: Modeling study of regional severe hazes over mid-eastern China in January 2013 and its implications on pollution prevention and control, *Sci. China Earth Sci.*, 57, 3–13, 2014.

Wendisch, M., Hellmuth, O., Ansmann, A., Heintzenberg, J., Engelmann, R., Althausen, D., Eichler, H., Mueller, D., Hu, M., and Zhang, Y.: Radiative and dynamic effects of absorbing aerosol particles over the Pearl River Delta, China, *Atmos. Environ.*, 42, 6405–6416, 2008.

Xing, L., Fu, T.-M., Cao, J. J., Lee, S. C., Wang, G. H., Ho, K. F., Cheng, M.-C., You, C.-F., and Wang, T. J.: Seasonal and spatial variability of the OM/OC mass ratios and high regional correlation between oxalic acid and zinc in Chinese urban organic aerosols, *Atmos. Chem. Phys.*, 13, 4307–4318, doi:10.5194/acp-13-4307-2013, 2013.

Xu, J., Ma, J. Z., Zhang, X. L., Xu, X. B., Xu, X. F., Lin, W. L., Wang, Y., Meng, W., and Ma, Z. Q.: Measurements of ozone and its precursors in Beijing during summertime: impact of urban plumes on ozone pollution in downwind rural areas, *Atmos. Chem. Phys.*, 11, 12241–12252, doi:10.5194/acp-11-12241-2011, 2011.

Yang, F., Tan, J., Zhao, Q., Du, Z., He, K., Ma, Y., Duan, F., Chen, G., and Zhao, Q.: Characteristics of PM_{2.5} speciation in representative megacities and across China, *Atmos. Chem. Phys.*, 11, 5207–5219, doi:10.5194/acp-11-5207-2011, 2011.

Yang, K., Dickerson, R. R., Carn, S. A., Ge, C., and Wang, J.: First observations of SO₂ from the satellite Suomi NPP OMPS: widespread air pollution events over China, *Geophys. Res. Lett.*, 40, 4957–4962, 2013.

Yao, X. H., Chan, C. K., Fang, M., Cadle, S., Chan, T., Mulawa, P., He, K. B., and Ye, B. M.: The water-soluble ionic composition of PM_{2.5} in Shanghai and Beijing, China, *Atmos. Environ.*, 36, 4223–4234, doi:10.1016/s1352-2310(02)00342-4, 2002.

Exploring the severe winter haze in Beijing

G. J. Zheng et al.

Title Page

Abstract

Introduction

Conclusions

References

Tables

Figures



Back

Close

Full Screen / Esc

Printer-friendly Version

Interactive Discussion



York, D., Evensen, N. M., Martinez, M. L., and Delgado, J. D.: Unified equations for the slope, intercept, and standard errors of the best straight line, *Am. J. Phys.*, 72, 367–375, doi:10.1119/1.1632486, 2004.

Zhang, J. K., Sun, Y., Liu, Z. R., Ji, D. S., Hu, B., Liu, Q., and Wang, Y. S.: Characterization of submicron aerosols during a month of serious pollution in Beijing, 2013, *Atmos. Chem. Phys.*, 14, 2887–2903, doi:10.5194/acp-14-2887-2014, 2014.

Zhang, Q., Streets, D. G., Carmichael, G. R., He, K. B., Huo, H., Kannari, A., Klimont, Z., Park, I. S., Reddy, S., Fu, J. S., Chen, D., Duan, L., Lei, Y., Wang, L. T., and Yao, Z. L.: Asian emissions in 2006 for the NASA INTEX-B mission, *Atmos. Chem. Phys.*, 9, 5131–5153, doi:10.5194/acp-9-5131-2009, 2009.

Zhao, P. S., Zhang, X. L., Xu, X. F., and Zhao, X. J.: Long-term visibility trends and characteristics in the region of Beijing, Tianjin, and Hebei, China, *Atmos. Res.*, 101, 711–718, doi:10.1016/j.atmosres.2011.04.019, 2011.

Zhao, X. J., Zhang, X. L., Xu, X. F., Xu, J., Meng, W., and Pu, W. W.: Seasonal and diurnal variations of ambient PM_{2.5} concentration in urban and rural environments in Beijing, *Atmos. Environ.*, 43, 2893–2900, doi:10.1016/j.atmosenv.2009.03.009, 2009.

Zhao, X. J., Zhao, P. S., Xu, J., Meng, W., Pu, W. W., Dong, F., He, D., and Shi, Q. F.: Analysis of a winter regional haze event and its formation mechanism in the North China Plain, *Atmos. Chem. Phys.*, 13, 5685–5696, doi:10.5194/acp-13-5685-2013, 2013.

Zheng, B., Zhang, Q., Zhang, Y., He, K. B., Wang, K., Zheng, G. J., Duan, F. K., Ma, Y. L., and Kimoto, T.: Heterogeneous chemistry: a mechanism missing in current models to explain secondary inorganic aerosol formation during the January 2013 haze episode in North China, *Atmos. Chem. Phys. Discuss.*, 14, 16731–16776, doi:10.5194/acpd-14-16731-2014, 2014.

Zheng, G., Cheng, Y., He, K., Duan, F., and Ma, Y.: A newly identified calculation discrepancy of the Sunset semi-continuous carbon analyzer, *Atmos. Meas. Tech. Discuss.*, 7, 377–399, doi:10.5194/amtd-7-377-2014, 2014.

Zhou, J. M., Zhang, R. J., Cao, J. J., Chow, J. C., and Watson, J. G.: Carbonaceous and ionic components of atmospheric fine particles in Beijing and their impact on atmospheric visibility, *Aerosol Air Qual. Res.*, 12, 492–502, doi:10.4209/aaqr.2011.11.0218, 2012.

Exploring the severe winter haze in Beijing

G. J. Zheng et al.

Title Page

Abstract

Introduction

Conclusions

References

Tables

Figures



Back

Close

Full Screen / Esc

Printer-friendly Version

Interactive Discussion

**Table 1.** General information on severe haze episodes in January 2013.

		Episode I			Episode II			Episode III			Jan		
		Ave.	min	max	Ave.	min	max	Ave.	min	Max	Ave.	min	max
Meteorology Data	Temperature (°C)	-4.63	-11.10	1.40	-2.79	-8.30	2.80	-1.26	-6.60	5.00	-2.94	-12.50	5.00
	RH (%)	31.16	13.50	58.50	56.59	27.20	77.60	55.05	27.10	79.70	47.97	13.50	88.30
	WS (m s ⁻¹)	2.10	0.90	4.40	2.08	1.00	3.40	1.96	0.90	3.60	2.18	0.90	4.50
PM _{2.5} and PM ₁₀	PM _{2.5} (µg m ⁻³)	112.50	11.00	311.50	245.37	21.10	855.10	167.66	35.40	387.30	161.77	4.40	855.10
	PM ₁₀ (µg m ⁻³)	152.17	28.80	411.00	327.17	31.60	1157.50	214.03	41.50	479.80	223.53	13.90	1157.50
	PM _{2.5} /PM ₁₀ (%)	0.69			0.75			0.79			0.70		
Gas Data	NO ₂	76.39			109.44			95.86			86.09		
	SO ₂	79.73			123.35			63.86			77.54		

Exploring the severe winter haze in Beijing

G. J. Zheng et al.

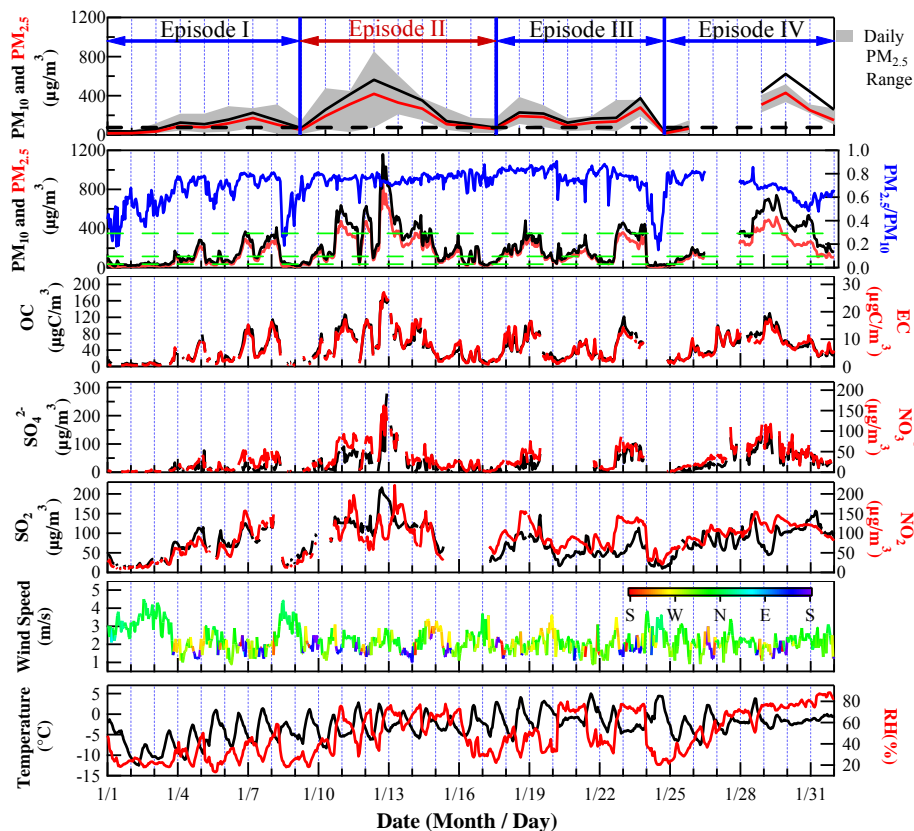


Figure 1. Time series of PM_{10} , $PM_{2.5}$, and its major components (OC, EC, SO_4^{2-} and NO_3^-), and meteorological data (wind speed, wind direction, temperature and relative humidity) for January 2013.

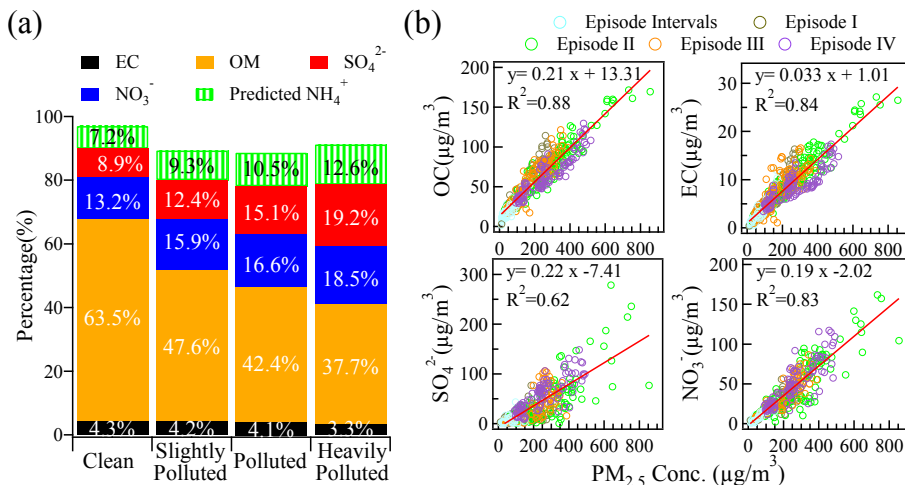


Figure 2. Percentile composition of major components in PM_{2.5} with respect to (a) pollution level and (b) PM_{2.5} mass concentration.

Title Page

Abstract

Introduction

Conclusions

References

Tables

Figures

◀

▶

◀

▶

Back

Close

Full Screen / Esc

Printer-friendly Version

Interactive Discussion



Exploring the severe winter haze in Beijing

G. J. Zheng et al.

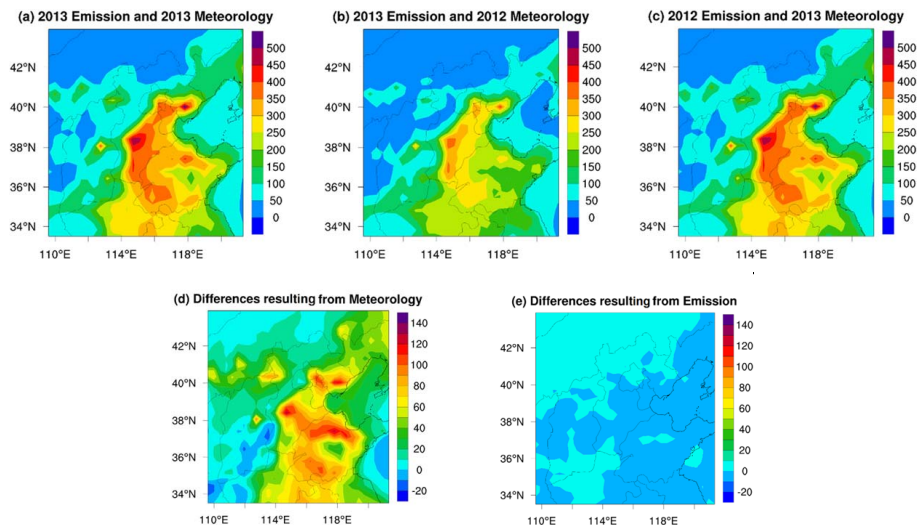


Figure 3. Model simulation results under different scenarios. **(a)** Base scenario. Actual 2013 emission and 2013 meteorology data were used. **(b)** 2012 meteorology data were used, and **(c)** 2012 emissions were used. The difference caused by meteorology **(d)**; equivalent to **a–b**) and emission **(e)**, equivalent to **a–c**) is also shown.

Exploring the severe winter haze in Beijing

G. J. Zheng et al.

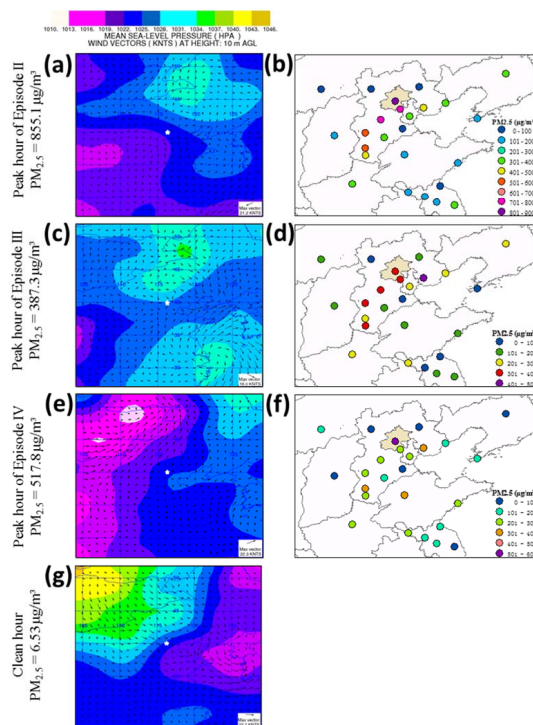


Figure 4. Surface weather maps (a, c, e, g) and PM_{2.5} concentrations (b, d, f) of the North China Plain on 12 January LT 18:00 (a, b), 18 January LT 20:00 (c, d), 29 January LT 13:00 (e, f), and 1 January LT 8:00 (g). The location of Beijing is indicated as a white star on the weather maps, and as the shaded area on the PM_{2.5} concentration maps. PM_{2.5} concentrations in Beijing at the four selected time points are also shown on the left for reference.

Exploring the severe winter haze in Beijing

G. J. Zheng et al.

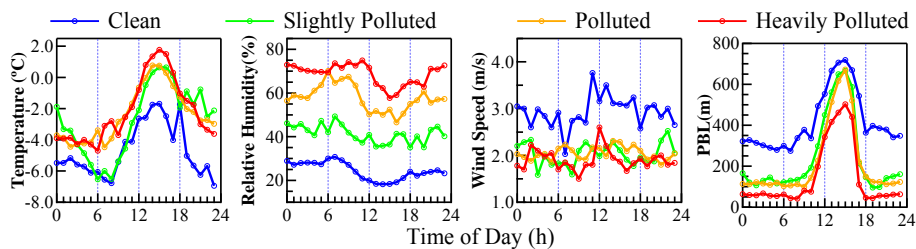


Figure 5. Diurnal variation in meteorological parameters for different pollution levels.

[Title Page](#)[Abstract](#)[Introduction](#)[Conclusions](#)[References](#)[Tables](#)[Figures](#)[◀](#)[▶](#)[◀](#)[▶](#)[Back](#)[Close](#)[Full Screen / Esc](#)[Printer-friendly Version](#)[Interactive Discussion](#)

Exploring the severe winter haze in Beijing

G. J. Zheng et al.

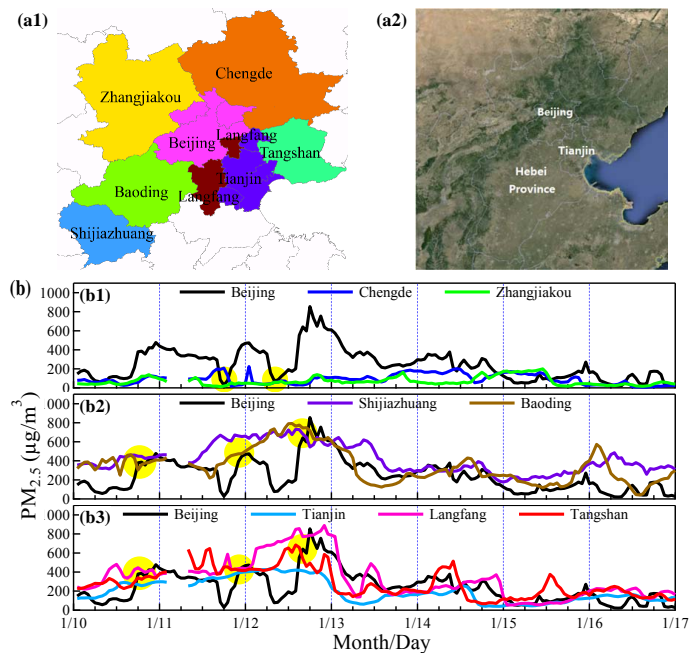


Figure 6. (a1) The location of all cities shown below, and (a2) topographic map around Beijing. (b) PM_{2.5} concentrations of Beijing and its (b1) northern cities, (b2) southwest cities, and (b3) southeast cities for the period 10–17 January 2013. Yellow solid circles indicated the time periods when the sharp drops (b1) and sharp increases (b2 and b3) of PM_{2.5} concentration occurred.



Exploring the severe winter haze in Beijing

G. J. Zheng et al.

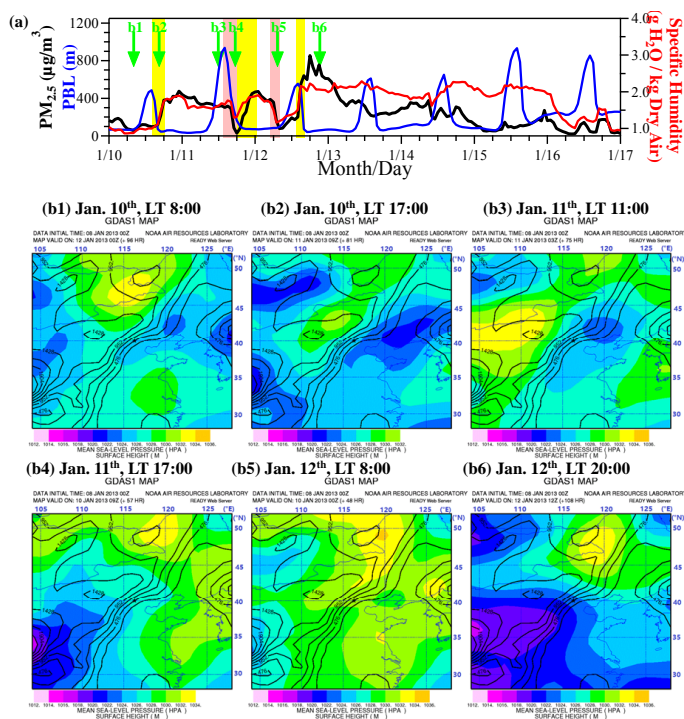


Figure 7. Evidence for regional transport of pollutants as a major factor contributing to sharp concentration increases in Beijing. **(a)** $PM_{2.5}$ concentration, PBL height, and specific humidity in Beijing for 10–17 January 2013. Pink and yellow rectangles indicated the sharp drop and sharp increase periods of $PM_{2.5}$, respectively. Note how nicely specific humidity and $PM_{2.5}$ followed each other during these periods. **(b)** Weather patterns before and after the sharp increases events. Corresponding time point of **(b1)** to **(b6)** was indicated by arrows in **(a)**. The topography map (elevation) is also shown for reference. Location of Beijing was indicated by the black star in center of each graph.

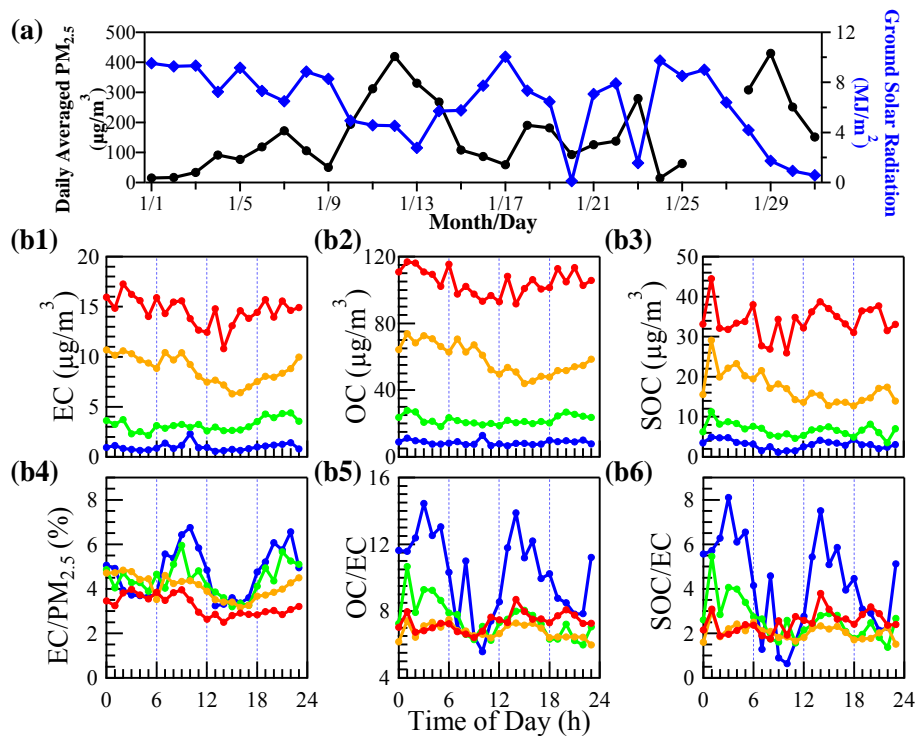


Figure 8. (a) Change in solar radiation and $PM_{2.5}$ concentration. (b) Change in diurnal pattern of OC, EC and SOC concentrations, percentage contribution of EC to $PM_{2.5}$, OC/EC and SOC/EC for different pollution levels.

Exploring the severe winter haze in Beijing

G. J. Zheng et al.

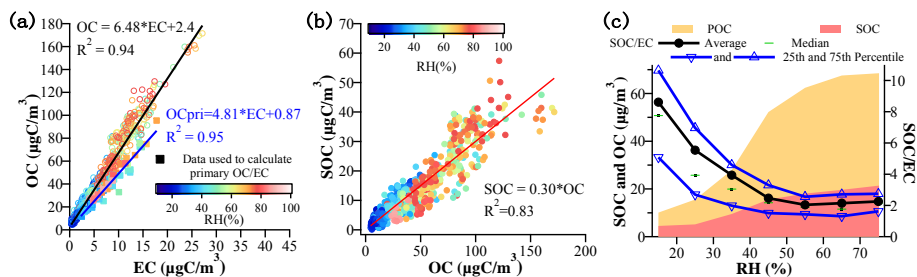


Figure 9. Estimation and implications of SOC formation. **(a)** Estimation of SOC with EC-tracer method. **(b)** SOC plotted against OC, colored with RH. **(c)** Change of SOC, OC and SOC/EC with RH.

Exploring the severe winter haze in Beijing

G. J. Zheng et al.

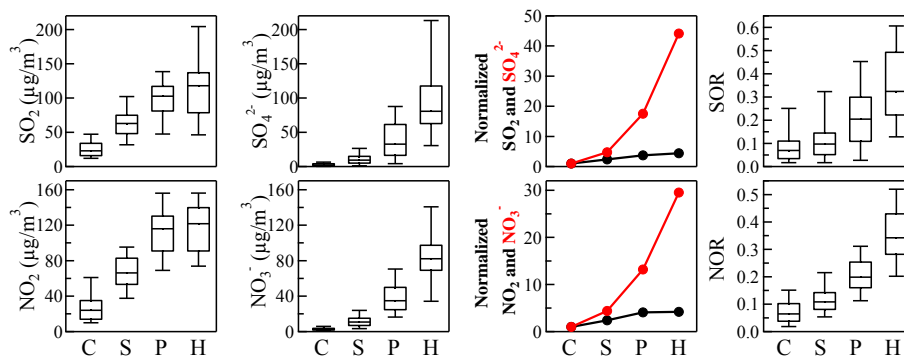


Figure 10. Variation of SO_2 , NO_2 , SOR, NOR, SO_4^{2-} and NO_3^- with pollution level. “C”, “S”, “P”, “H” refer to “clean”, “slightly polluted”, “polluted” and “heavily polluted”, respectively. Normalized X in Column 3 refers to the average concentration of X in any pollution level, scaled by its average concentration during clean periods.

Title Page

Abstract

Introduction

Conclusions

References

Tables

Figures



Back

Close

Full Screen / Esc

Printer-friendly Version

Interactive Discussion



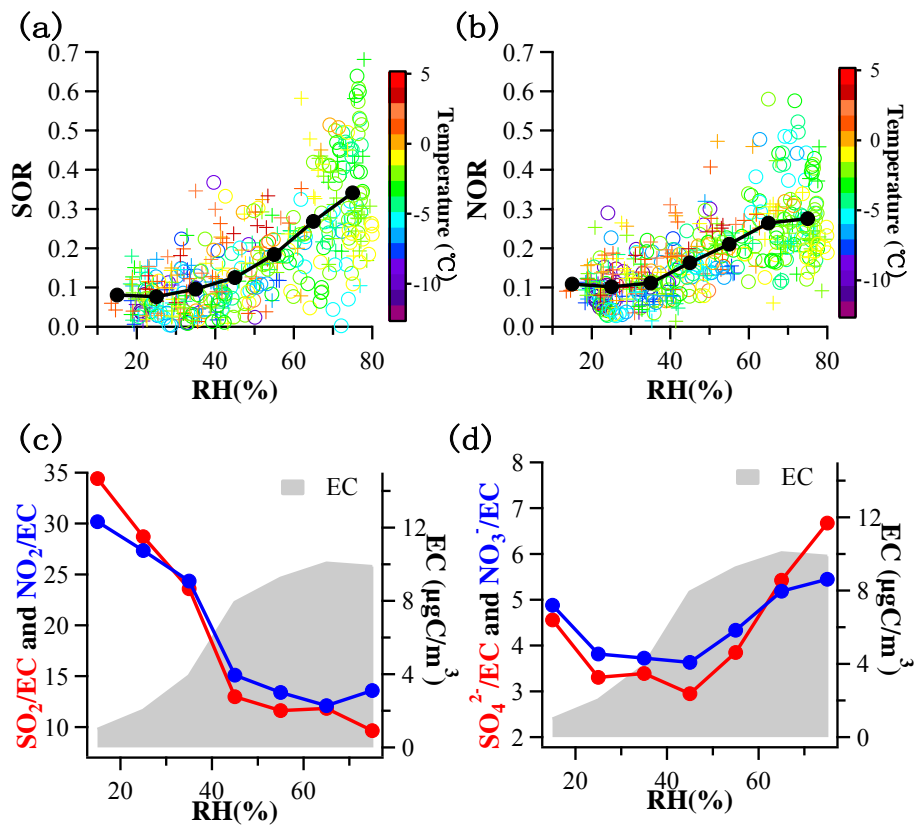


Figure 11. Importance of heterogeneous chemistry in sulfate and nitrate formation. **(a–b)** SOR and NOR plotted against RH, colored with temperature. **(c–d)** EC-scaled precursors (SO₂ and NO₂) and product (SO₄²⁻ and NO₃⁻) plotted against RH. Change of EC concentration with RH level was also shown for reference.

Exploring the severe winter haze in Beijing

G. J. Zheng et al.

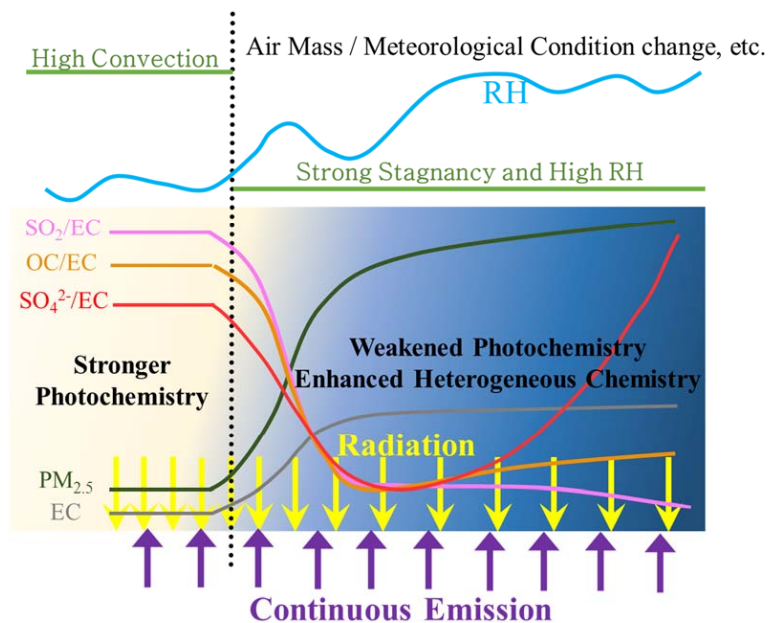


Figure 12. Conceptual model of atmospheric chemistry during the heavy pollutions. The dotted black line indicated the meteorology changed from convection-favoring condition to stagnant condition.

[Title Page](#)
[Abstract](#)
[Introduction](#)
[Conclusions](#)
[References](#)
[Tables](#)
[Figures](#)
[Back](#)
[Close](#)
[Full Screen / Esc](#)
[Printer-friendly Version](#)
[Interactive Discussion](#)